Inorganic Chemistry

Article

pubs.acs.org/IC

Coordination of a Hemilabile Pincer Ligand with an Olefinic Backbone to Mid-to-Late Transition Metals

Brittany J. Barrett and Vlad M. Iluc*

Department of Chemistry and Biochemistry, University of Notre Dame, 251 Nieuwland Science Hall, Notre Dame, Indiana 46556, United States

Supporting Information

ABSTRACT: The coordination chemistry of a neutral *t*PCH═CHP pincer (*t*PCH═CHP = 2,2′-bis(di-*iso*-propylphosphino)-*trans*-stilbene) with metals that form stable complexes in the +1 oxidation state was studied and (*t*PCH═CHP)CoCl, (*t*PCH═CHP)CoCl(CO), (*t*PCH═CHP)RhCl, (*t*PCH═CHP)Cu(OTf), [(*t*PCH═CHP)Cu][PF_6], and [(*t*PCH═CHP)Ag][PF_6] were synthesized and characterized. In order to determine whether the coordination mode is dependent on the oxidation state of the metal, some +2 metal complexes, (*t*PCH═CHP)$CoCl_2$ and (*t*PCH═CHP)$FeBr_2$, were also investigated. The coordination of the olefinic backbone is not observed in (*t*PCH═CHP)$FeBr_2$, (*t*PCH═CHP)$CoCl_2$, (*t*PCH═CHP)Cu(OTf), or [(*t*PCH═CHP)Ag][PF_6], but η^2-coordination is present in [(*t*PCH═CHP)CoCl][$BAr^F{}_4$], [(*t*PCH═CHP)FeBr][$BAr^F{}_4$], (*t*PCH═CHP)CoCl, (*t*PCH═CHP)CoCl(CO), (*t*PCH═CHP)RhCl, and [(*t*PCH═CHP)Cu][PF_6]. Cobalt(II), iron(II), and copper(I) formed complexes with the ligand in both coordination modes. All metal complexes were characterized by multinuclei NMR spectroscopy, X-ray crystallography, and elemental analysis.

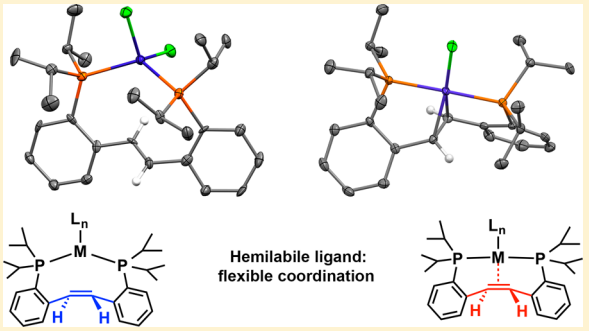

INTRODUCTION

Recent work in organometallic chemistry has focused on designing ancillary ligands that may participate in reactions at the metal center.[1−7] A related type of metal−ligand cooperation that has been known by coordination chemists for some time is that of hemilabile ligands,[8−17] when multidentate chelating ligands are employed. Depending on certain electronic requirements of the metal center and the reaction environment, one of the arms of the supporting ligand may dissociate and, thus, accommodate reactivity behaviors not observed in the absence of such mechanisms.[12,18] An elegant study of similar interactions was recently reported by the Peters group and has bearings on the fact that a single Fe-binding site of the nitrogenase cofactor may mediate N_2 reduction catalysis by invoking a hemilabile role for the interstitial carbon atom.[19]

Pincers represent a versatile class of ligands with various examples of metal−ligand cooperation reported.[20−23] In addition, the corresponding metal complexes tend to be stable and robust.[24,25] Many examples include a central, anionic, strong σ donor flanked by two neutral groups. Recent examples, in which the central chelating moiety is neutral, have been featuring a pyridine or a phosphine group.[26,27] Interestingly, such ligands show a different coordination mode depending on various factors such as the type of metal or its oxidation state.[26,27] For example, pyridine-based PNP ligands (2,6-bis(phosphinomethyl)pyridine) showed hemilabile characteristics upon coordination to a copper metal center (Figure 1).[26] It was found that, in the presence of bromide, the pyridine nitrogen is dissociated from the metal center; bromide extrusion with a silver salt led to pyridine coordination, stabilizing the complex (Figure 1).[26] These PNP ligands also have the ability to undergo reversible charge switching by transferring a hydrogen atom to the metal while the central pyridine moiety can act as either a neutral or anionic moiety. This is a feature that has led to interesting reactivity toward small molecule activation and water splitting as reported by the Milstein group.[28]

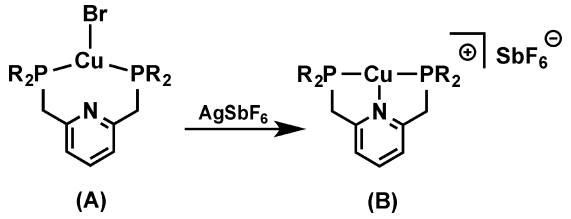

Figure 1. Hemilabile characteristics of a neutral PNP ligand (adapted from ref 26): (A) weak Cu—N interaction, Cu—N distance is 2.89 Å, (B) strong Cu—N interaction, Cu—N distance is 2.09 Å.

We became interested in determining whether a neutral ligand including an alkene as the central chelating moiety, PCH═CHP, would act in a hemilabile manner and change its coordination mode from noncoordination to η^2-coordination. Bennett and co-workers initially observed κ^4-PCCP coordina-

Received: March 10, 2014
Published: June 24, 2014

   dx.doi.org/10.1021/ic500549z | *Inorg. Chem.* 2014, 53, 7248−7259

tion of 2,2′-bis(diphenylphosphino)-*trans*-stilbene[29−31] with group 6 and 9 metals in the 0 and +1 oxidation state, respectively (Figure 2). Furthermore, we reported a study of

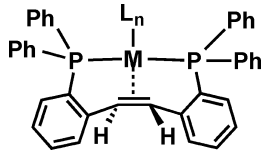

Figure 2. Coordination of 2,2′-bis(diphenylphosphino)-*trans*-stilbene to group 6 and 9 metals.

group 10 metal complexes describing the coordination modes of *t*PCH═CHP and C—H activation of the olefinic backbone.[32] Herein, we report an in-depth investigation of the coordination chemistry of 2,2′-bis(di-*iso*-propylphosphino)-*trans*-stilbene by studying iron, cobalt, rhodium, copper, and silver complexes in a variety of oxidation states. Complementary to the results previously reported by the Bennett group, who studied only rhodium(I) and iridium(I) complexes, we observe more than one coordination mode with a metal center depending on its oxidation state or electronic requirements.

RESULTS AND DISCUSSION

Compound 2,2′-bis(di-*iso*-propylphosphino)-*trans*-stilbene (*t*PCH═CHP, **1**)[32] differs from 2,2′-bis(diphenylphosphino)-*trans*-stilbene in that the phenyl phosphine groups are replaced with *iso*-propyls. We hypothesized that this modification would lead to increased solubility of the resulting metal complexes and allow us to survey various oxidation states of the same metal.

First, metals in the +2 oxidation state were studied. The formation of (*t*PCH═CHP)$CoCl_2$ (**2**) was observed upon mixing **1** with $CoCl_2$ in THF (Scheme 1). The paramagnetic product was characterized by single crystal X-ray diffraction (Figure 3), which showed a pseudotetrahedral geometry[33−38] around the metal center with angles ranging from 98.09(6)° to

Scheme 1. Synthesis of Complexes 2−5

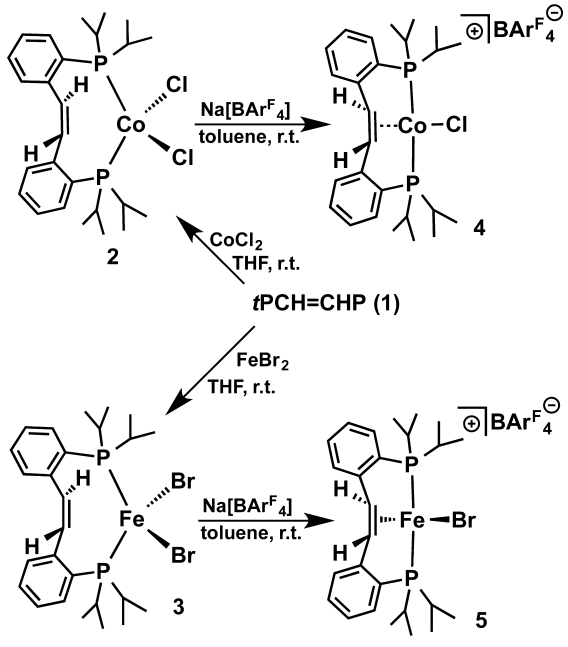

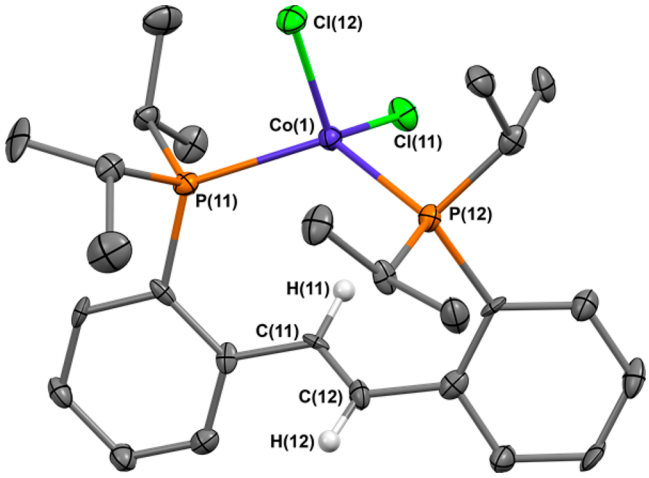

Figure 3. Thermal-ellipsoid (50% probability level) representation of (*t*PCH═CHP)$CoCl_2$ (**2**). Only one of the two crystallographically independent molecules is shown. Most hydrogen atoms were omitted for clarity. Selected distances (Å) and angles (deg): Co(1)—P(11) = 2.4305(17), Co(1)—P(12) = 2.4236(18), Co(1)—Cl(11) = 2.2443(18), Co(1)—Cl(12) = 2.547(17), C(11)—C(12) = 1.317(8), P(11)—Co(1)—P(22) = 126.44(7), P(11)—Co(1)—Cl(11) = 105.66(6), P(12)—Co(1)—Cl(1) = 105.12(7), Cl(11)—Co(1)—Cl(12) = 116.59(8), P(11)—Co(1)—Cl(12) = 98.09(6), P(12)—Co(1)—Cl(12) = 105.73(7).

126.44(7)°. Compound **2** exhibits a noncoordinated olefinic backbone that retains C═C double bond character, as indicated by the C—C distance of 1.317(8) Å (Figure 3). Additionally, the average distance of 3.501 Å from cobalt to the centroid of the olefin supports this interpretation. Other metrical parameters compare well with those previously reported: the Co—P distances in **2** (2.4236(18) and 2.4305(17) Å) are long compared to typical Co—P distances (2.1−2.3 Å),[39−41] but a similar situation was observed before: 2.369(5) Å in [$(Cy_3P)Co(dmgH)_2Cl$] (dmgH = dimethylglyoximate), 2.418(1) Å in [$(Ph_3P)Co(dmgH)_2(CH_3)$],[42] 2.520(2) Å in [$CoL_2(O_3SCF_3)_2$] (L = $P(CH_2Ph)(CH_2CH_2OC_2H_5)_2$,[43] and 2.3666(14), 2.3731(15) Å in a Co(II) tetrahedral complex supported by a P—N—P ligand, $CH_3N(CH_2CH_2PPh_2)_2$.[39] In the first three examples, the lengthening of Co—P distances was attributed to the *trans* effect of other ligands. However, such an explanation is not applicable to the P—N—P case, as well as ours, since the potentially tridentate ligand acts only in a bidentate manner, coordinating solely through the two phosphines. This elongation can be partially attributed to the steric bulk of the phosphine donors in both cases, but other factors may play an additional role. In {$CH_3N(CH_2CH_2PPh_2)_2$}$CoCl_2$, it was proposed that although the cobalt complex is electron deficient (15 electron count), coordination of the nitrogen donor does not occur as a result of the steric effect of the methyl nitrogen substituent and the relatively low coordinating ability of the tertiary nitrogen. In **2**, it is also possible that the tetrahedral geometry is favored over a square-pyramidal or trigonal-bipyramidal geometry that would result upon olefin coordination.[44]

In order to determine whether the lack of olefin coordination is a characteristic of metals in the +2 oxidation state, the reaction of **1** with $FeBr_2$ (Scheme 1) in THF was carried out and resulted in the formation of an orange solution. Upon removal of volatiles and trituration with *n*-pentane, a pure tan

dx.doi.org/10.1021/ic500549z | *Inorg. Chem.* 2014, 53, 7248−7259

solid, identified as (*t*PCH═CHP)$FeBr_2$, **3**, was obtained. ^{1}H NMR spectroscopy showed the formation of a paramagnetic product, which was also supported by the lack of signals in the corresponding ^{31}P NMR spectra. Single crystal X-ray diffraction was used to characterize **3** (Figure 4), indicating a

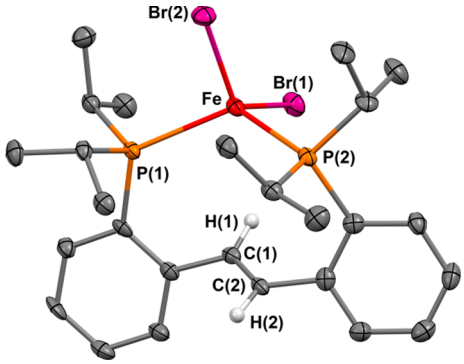

Figure 4. Thermal-ellipsoid (50% probability level) representation of (*t*PCH═CHP)$FeBr_2$ (**3**). Most hydrogen atoms were omitted for clarity. Selected distances (Å) and angles (deg): C(1)cC(2) = 1.320(6), Fe—P(1) = 2.5209(13), Fe—P(2) = 2.5232(14), Fe—Br(2) = 2.4038(8), Fe—Br(1) = 2.4096(8), Br(1)—Fe—Br(2) = 122.62(3), Br(1)—Fe—P(2) = 103.22(4), Br(1)—Fe—P(1) = 107.88(4), Br(2)—Fe—P(1) = 98.91(4), Br(2)—Fe—P(2) = 103.30(4), P(1)—Fe—P(2) = 122.45(5).

pseudotetrahedral geometry around iron[45,46] with angles in the 98.91(4)−122.62(3)° range. The distortion observed (angles smaller or larger than the ideal value, 104.5°) may be attributed to the relative rigidity of the *t*PCH═CHP backbone. The solid state molecular structure is also consistent with a noncoordinated olefinic moiety in **3**, with a 3.596 Å distance from the metal center to the centroid of the C═C bond. The Fe—P distances of 2.5232(14) and 2.5209(13) Å are slightly elongated compared to previously reported Fe—P values,[47,48] likely the result of the relative rigidness of the backbone coupled with steric crowding around the metal center.

Since we are interested in the hemilabile behavior of *t*PCH═CHP, we reasoned that abstraction of a halide ligand from **2** and **3** would render the metal center more electron poor and induce coordination of the olefinic backbone. Consequently, compounds **2** and **3** were treated with sodium tetrakis[3,5-bis(trifluoromethyl)phenyl]borate ($NaBAr^F_4$). After 12 h, the formation of new paramagnetic products, [(*t*PCH═CHP)-CoCl][BAr^F_4] (**4**) and [(*t*PCH═CHP)FeBr][BAr^F_4] (**5**), respectively, was observed as indicated by broad ^{1}H NMR spectra and the absence of peaks in the corresponding ^{31}P NMR spectra.

Analysis of complex **4** by ^{11}B and ^{19}F NMR spectroscopy confirmed the incorporation of the BAr^F_4 counterion. Crystallization from a concentrated toluene solution layered with *n*-pentane yielded crystals suitable for X-ray diffraction. The solid state molecular structure (Figure 5) shows the formation of a pseudo-square-planar complex, in which the abstraction of one chloride ligand led to the coordination of the olefinic moiety. The square-planar geometry is also supported by the observed magnetic moment of 1.8 μ_B, corresponding to one unpaired electron. Examples of cobalt(II) square-planar complexes are rare. In general, tetrahedral examples are found when two of the ligands are halides, such as in the species reported by Wang et al., in which a PNP ligand, $CH_3N(CH_2CH_2PPh_2)_2$, binds to the metal center through the

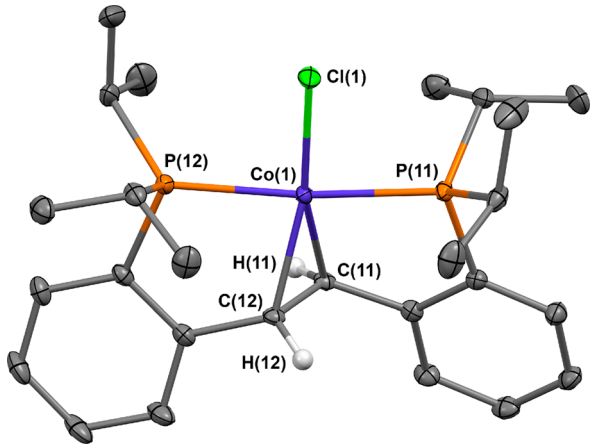

Figure 5. Thermal-ellipsoid (50% probability level) representation of [(*t*PCH═CHP)CoCl][BAr^F_4] (**4**). Only one of the two crystallographically independent cations is shown. Most hydrogen atoms were omitted for clarity. Selected distances (Å) and angles (deg): Co(1)—P(11) = 2.2536(12), Co(1)—P(12) = 2.2546(12), Co(1)—Cl(1) = 2.2020(11), C(11)—C(12) = 1.397(6), P(11)—Co(1)—P(12) = 172.09(5), P(11)—Co(1)—Cl(1) = 86.45(4), P(12)—Co(1)—Cl(1) = 85.84(4).

phosphine moieties while the amine functionality remains dissociated. In that example, two chloride ligands are also bound to the metal center.[39] Similarly, Alyea et al. also report a tetrahedral cobalt(II) species in which the metal center is bound in a κ^2-P,P fashion to a PSiP ligand, $Ph_2PCH_2Si(CH_3)_2CH_2PPh_2$, as well as two bromide ligands.[49] Square-planar cobalt(II) examples have been reported by the Arnold group,[50] who described a neutral complex containing a PNP ligand, κ^3-P,N,P—$N(CH_2CH_2P^iPr_2)_2$, coordinated in a tridentate mode to a cobalt(II) center containing also a chloride ligand. Protonation of the supporting ligand led to a cationic cobalt(II) species that retained the square-planar geometry.[50] In our complex, the P(11)—Co—P(12) angle of 172.09(5)° and the P(11)—Co—Cl(1) angle of 85.84(4)° support the assignment of the pseudo-square-planar geometry. The C(11)—C(12) distance of 1.397(6) Å is only mildly elongated for a C—C double bond, indicating that the amount of backdonation to the alkene is limited as expected for a cationic compound.

Similarly to complex **4**, the iron(II) species [(*t*PCH═CHP)FeBr][BAr^F_4] (**5**) contained the BAr^F_4 counterion as indicated by ^{11}B and ^{19}F NMR spectroscopy. Crystals suitable for single crystal X-ray diffraction were obtained from a concentrated toluene solution layered with *n*-pentane, and illustrate the formation of a pseudotetrahedral iron(II) complex as indicated by the angles ranging from 111.93(2)° to 121.38(3)° (Figure 6). Distortions in the geometry are attributed to the relative rigidity of the ligand. Analogous to **4**, the olefin coordinates upon halide abstraction and does not experience a significant amount of π-backbonding from the metal center (C(1)—C(2) distance is 1.332(14) Å). To the best of our knowledge, four-coordinate iron(II) complexes tend to exhibit tetrahedral geometries more often than square-planar.[51−53] The Chirik group investigated the preference for a square-planar versus tetrahedral geometry for iron(II) complexes, and observed that steric factors tend to outweigh the electronic stabilization offered by the square-planar geometry when chelating amines are employed.[48] Chelating phosphine ligands were, however, less straightforward cases, but the

dx.doi.org/10.1021/ic500549z | *Inorg. Chem.* 2014, 53, 7248−7259

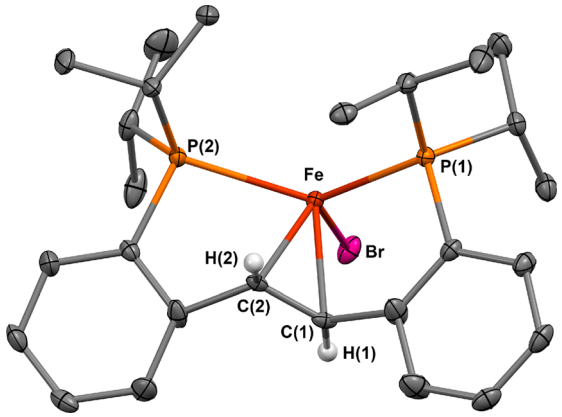

Figure 6. Thermal-ellipsoid (50% probability level) representation of [(*t*PCH═CHP)FeBr][BAr^F_4] (**5**). Most hydrogen atoms were omitted for clarity. Selected distances (Å) and angles (deg): C(1)—C(2) = 1.332(14), Fe—P(1) = 2.4312(7), Fe—P(2) = 2.4220(7), Fe—Br = 2.3213(5), Br—Fe—P(1) = 115.41(2), Br—Fe—P(2) = 111.93(2), P(1)—Fe—P(2) = 121.38(3).

preference for a specific geometry appeared to be related to the ligand field strength. Halides used in conjunction with chelating phosphines led to tetrahedral iron complexes.[48] It is likely that similar considerations apply to the observed tetrahedral geometry of **5**.

A cobalt(I) complex, (*t*PCH═CHP)CoCl (**6**), was obtained upon reduction of **2** with 0.25 equiv of $LiAlH_4$ (Scheme 2).

Scheme 2. Synthesis of Complexes 6 and 7

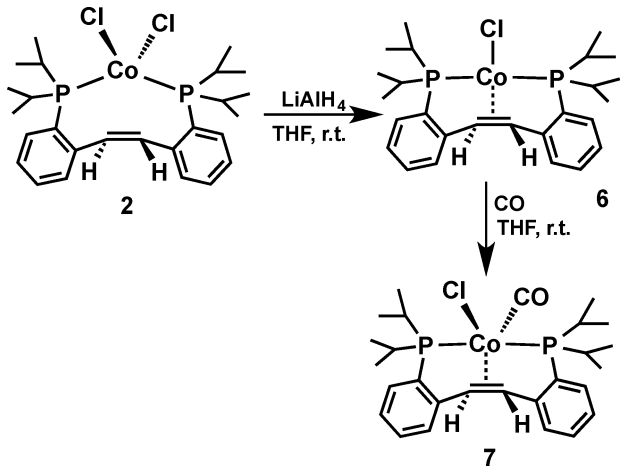

The ^{31}P NMR spectrum of **6** exhibits a broad singlet at 51.08 ppm consistent with equivalent phosphorus environments. Notably, the corresponding ^{1}H NMR spectrum shows a significant upfield shift of the olefinic protons to 2.01 ppm from those values in *t*PCH═CHP (8.53 ppm). This shift is consistent with a bound olefinic moiety and a considerable amount of π backbonding from the metal center. The solid state molecular structure of **6** (Figure 7) agrees with this interpretation by showing an elongated C(1)—C(2) backbone distance of 1.442(5) Å and a pseudo-square-planar geometry of the cobalt center. Notably, this is longer than the Co(II) bound olefinic C—C distance observed for complex **4** (1.397(6) Å). This difference is attributed the higher degree of π-back-donation for complex **6** compared to the less electron rich complex **4**. Interestingly, the Co—P distances are similar in **6**

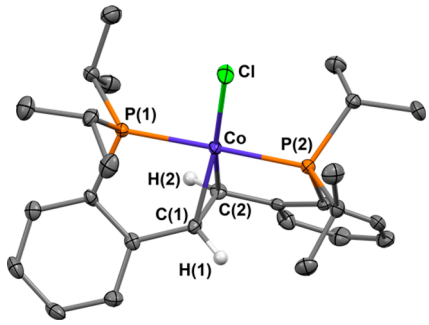

Figure 7. Thermal-ellipsoid (50% probability level) representation of (*t*PCH═CHP)CoCl (**6**). Most hydrogen atoms were omitted for clarity. Selected distances (Å) and angles (deg): Co—P(1) = 2.2138(11), Co—P(2) = 2.2145(11), Co—Cl = 2.2193(11), C(1)—C(2) = 1.442(5), P(1)—Co—P(2) = 178.76(5), Cl—Co—P(1) = 90.51(4), Cl—Co—P(2) = 89.69(4).

(2.2138(11) and 2.2145(11) Å) and **4** (2.2536(12) and 2.2546(12) Å), but they are shorter than in **2** (2.4305(17) and 2.4236(18) Å), consistent with the presence of a π-acceptor ligand in the former two complexes. The olefin was found in a near perpendicular orientation to the plane defined by P(1), Co(1), and P(2) with a dihedral angle of 78°, a feature reminiscent of Zeise's salt.[54−56] A cobalt(I) structure, previously reported by Grützmacher and co-workers, Co(tropp^{Ph})Cl(PPh_3) (tropp^{Ph} = tropylidene diphenylphosphine), contains a tetrahedral environment composed of two phosphine ligands, an olefin, and a chloride.[44] The difference in geometries for Co(tropp^{Ph})Cl(PPh_3) and **6** is likely a consequence of the rigidity of our ligand system, as well as the steric demands of the previously reported system. The broadness of the peaks observed in its ^{1}H as well as ^{31}P NMR spectra for complex **6** could be due to the presence of an equilibrium in solution between structures in which the metal center exists in a tetrahedral or a square-planar environment.[57] The equilibrium is shifted toward the square-planar species at low temperature, and a sharper ^{31}P NMR spectrum was observed at −70 °C.

In order to test the hemilability of the supporting ligand in **6**, the dissociation of the olefin moiety was targeted. The reaction of **6** with CO showed a rapid color change from deep purple to light orange. Examining the reaction mixture by ^{1}H NMR spectroscopy indicated the formation of a diamagnetic product, in which the olefinic protons display separate shifts at 3.64 and 4.68 ppm. The upfield shift of these protons compared to free ligand (8.52 ppm) indicates that the olefin remains bound to the metal center. ^{31}P NMR spectroscopy supports this observation, since peaks for two inequivalent phosphines, which exhibit a *trans*-coupling constant of 175 Hz, were observed. ^{13}C NMR spectroscopy confirms the presence of a CO ligand, with a corresponding chemical shift at 204.93 ppm. The olefinic carbon atoms are found upfield from free ligand (132.67 ppm) at 70.28 and 72.75 ppm, respectively, also consistent with the bound form of the alkene. Crystals suitable for single crystal X-ray diffraction were obtained from a concentrated solution of diethyl ether (Figure 8). The geometry of the complex was found to be trigonal-bipyramidal as indicated by the angles ranging from 101° to 115° for the trigonal plane defined by C(1)—C(2), Cl, and CO, as well as P(1)—Co—P(2) of 173.11(6)°. The C—C distance of the olefinic moiety is 1.438(7) Å, similar to the value observed for the starting material, **6**. The formation of **7** is analogous to

dx.doi.org/10.1021/ic500549z | *Inorg. Chem.* 2014, 53, 7248−7259

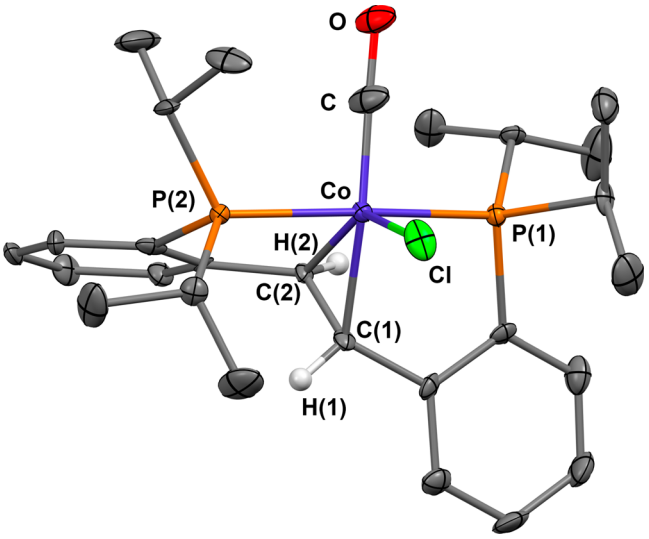

Figure 8. Thermal-ellipsoid (50% probability level) representation of (*t*PCH═CHP)CoCl(CO) (**7**). Most hydrogen atoms were omitted for clarity. Selected distances (Å) and angles (deg): Co—P(1) = 2.2378(14), Co—P(2) = 2.2495(14), Co—Cl = 2.348(5), C(1)—C(2) = 1.438(7), Co—C = 1.65(3), C—O = 1.18(4), P(1)—Co—P(2) = 173.11(6), Cl—Co—P(1) = 88.32(9), Cl—Co—P(2) = 92.49(10), Cl—Co—C = 101.2(7).

results reported by the Bennett group for reactions of rhodium(I) and iridium(I) complexes with CO[29] that led to trigonal-bipyramidal complexes in which the olefin remains bound.

A rhodium(I) complex analogous to **6**, (*t*PCH═CHP)RhCl (**8**), was obtained by reacting **1** with half an equivalent of rhodium cyclooctadiene chloride dimer ([(cod)RhCl]$_2$) in THF (eq 1). Similarly to **6**, the olefinic protons display an

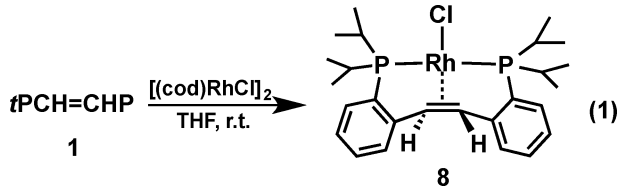

upfield shift to 3.74 ppm. The peak appears as a broad quartet; however, it is most likely an unresolved triplet of doublets due to coupling with the ^{103}Rh and ^{31}P nuclei. This complex is similar to the Rh(I) complex observed by Bennett with the phenyl analogue of the ligand, (bdpps)RhCl (bdpps = *o*-$Ph_2P—C_6H_4—CH═CH—C_6H_4—PPh_2$-*o*). In both instances, the olefin protons are shifted upfield in the ^{1}H NMR spectrum, a consequence of the bound olefin.[29] X-ray crystallography (Figure 9) indicated a square-planar complex,[58−61] with an elongated C(1)—C(1)# distance of 1.432(8) Å due to π-backbonding. The Rh—P distances of 2.2895(13) Å are similar to a previously reported square-planar PNP rhodium(I) complex, (PNP^{t}Bu)RhCl (PNP^{t}Bu = 2,6-bis(di-*tert*-butylphosphino-methyl)pyridine) (2.2−2.3 Å).[62,63] The olefin in the backbone approaches a perpendicular orientation to the plane defined by P(1), Rh(1), and P(1)# (dihedral angle of 73°), similarly to what was observed for compound **6**.

A copper(I) complex, (*t*PCH═CHP)CuI (**9**), was synthesized by stirring **1** with CuI at room temperature for 1 h (Scheme 3). The ^{1}H NMR spectrum for this complex shows

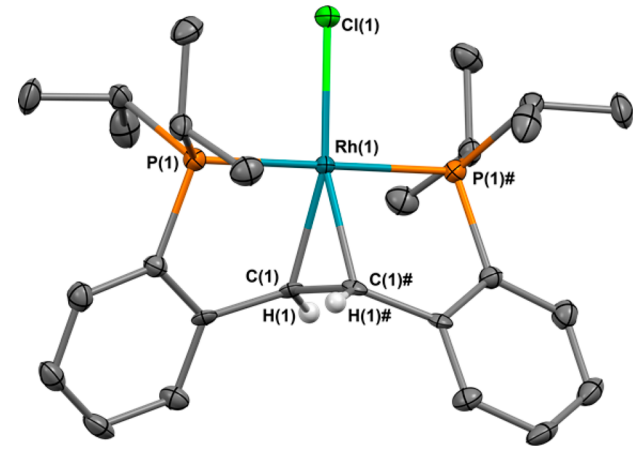

Figure 9. Thermal-ellipsoid (50% probability level) representation of **8**. Only one of the two crystallographically independent molecules is shown. Most hydrogen atoms were omitted for clarity. Selected distances (Å) and angles (deg): Rh(1)—P(1) = 2.2895(13), Rh(1)—Cl(1) = 2.3656(18), C(1)—C(1)# = 1.432(8), P(1)—Rh1—P(1)# = 179.88(7), Cl(1)—Rh(1)—P(1) = 90.07(6), Cl(1)—Rh(1)—P(1)# = 90.06(4).

Scheme 3. Synthesis of Complexes 9−11

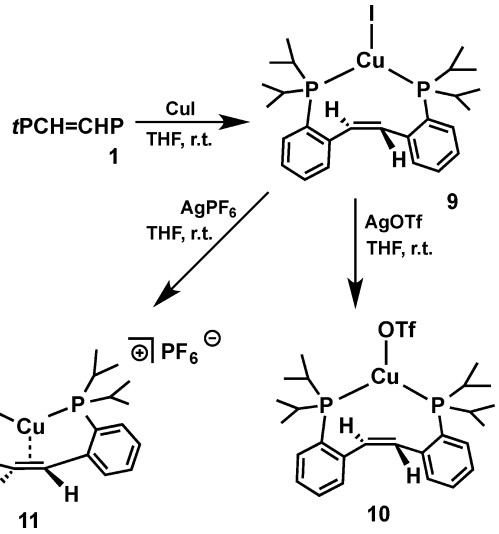

that the olefinic protons have a downfield chemical shift of 7.03 ppm indicating a noncoordinated backbone. A high degree of symmetry was found in the alkyl region that is also consistent with this interpretation: one environment for the four methine protons, with a signal at 2.50 ppm, and two environments for the eight methyl groups, at 1.25 and 1.34 ppm. The ^{31}P NMR spectrum of **9** also indicates equivalent environments for both phosphorus atoms (singlet at 7 ppm). We were unable to isolate single crystals suitable for X-ray diffraction for complex **9**. Therefore, the Cu(I) complex (*t*PCH═CHP)Cu(OTf) (**10**) was isolated from the reaction of **9** with AgOTf (Scheme 3). ^{1}H NMR spectroscopy indicates that the solution structure of **10** is similar to that of **9**: a downfield shift of 7.19 ppm for the olefinic protons and one environment for the four methine positions at 2.14 ppm are observed. The corresponding ^{31}P spectrum shows a singlet at 14.56 ppm, indicating that the phosphines are equivalent. Single crystals of **10** were obtained from a toluene solution layered with *n*-pentane. The solid state molecular structure (Figure 10) shows a pseudo-trigonal-planar

dx.doi.org/10.1021/ic500549z | Inorg. Chem. 2014, 53, 7248−7259

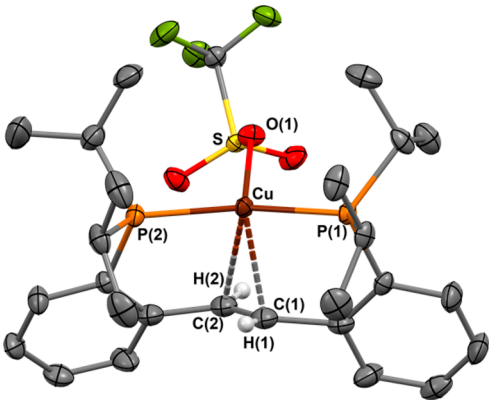

Figure 10. Thermal-ellipsoid (50% probability level) representation of **10**. Most hydrogen atoms were omitted for clarity. Selected distances (Å) and angles (deg): Cu—O(1) = 2.158(2), Cu—P(1) = 2.2137(8), Cu—P(2) = 2.2179(8), C(1)—C(2) = 1.294(5), Cu—C(1) = 2.370(3), Cu—C(2) = 2.644(3), O(1)—Cu—P(1) = 103.75(6), P(1)—Cu—P(2) = 149.23(3), O(1)—Cu—P(2) = 103.57(6).

coordination environment around copper[64] as indicated by angles ranging from 103.57(6)° to 149.23(3)° and a relatively close contact between the metal center and the olefin. The distance of 2.426 Å between copper and the olefinic backbone, however, is outside the range that indicates a strong bonding interaction and can be better explained as a weak interaction or a close contact. The olefinic C—C distance of 1.294(5) Å is consistent with a double bond that is not weakened by π-backdonation from the metal center. J. I. van der Vlugt and co-workers described a PNP Cu(I) system, (PNP^{tBu})CuBr and [(PNP^{tBu})Cu][SbF$_6$] (PNP^{tBu} = 2,6-bis[(di-*tert*-butylphosphino)methyl]pyridine), in which the geometry around the metal center is either trigonal-planar or T-shaped depending on the nature of the additional ligand.[26] In the trigonal-planar case, the metal center and the pyridine are in close contact; however, they are not considered to be bonding. Upon removal of bromide, the pyridine coordinates, resulting in a T-shaped complex (Figure 1).[26]

In an attempt to strengthen the coordination of the olefinic backbone to copper, removal of the iodide ligand utilizing AgPF$_6$ was undertaken and generated [(*t*PCH═CHP)Cu][PF$_6$] (**11**) (Scheme 3). There are several similarities between compounds **11** and **9** in their ^{1}H NMR spectra. The olefinic protons appear as a singlet at 7.02 ppm compared to 7.03 ppm for compound **9**, and the alkyl region is nearly identical for both compounds. The cationic nature of this compound is evident in its ^{31}P NMR spectrum, which shows a downfield shifted resonance at 25.41 ppm, compared to 7.00 ppm for compound **9**. The PF$_6^-$ counteranion is found upfield in the corresponding ^{31}P NMR spectrum at −143.28 ppm as a septet. The absence of upfield shifted olefinic protons is indicative of a lack of interaction with the metal center, behavior contrasting that of a previously observed copper(I) complex [(PNP^{tBu})Cu][SbF$_6$],[26] in which the central pyridine donor acted in a hemilabile fashion and dissociated in the presence of bromide.

The solid state molecular structure of **11** (Figure 11) elucidates the coordination environment of the copper(I) metal center. The geometry of the metal center is pseudo-T-shaped, as deduced from the P—Cu—P angle of 162.34(4)°. This angle is smaller than the corresponding angle in [(PNP^{tBu})Cu][SbF$_6$], which has a value of 172.44(3)°.[26] The olefin appears to be bound to the metal center; however the Cu—C

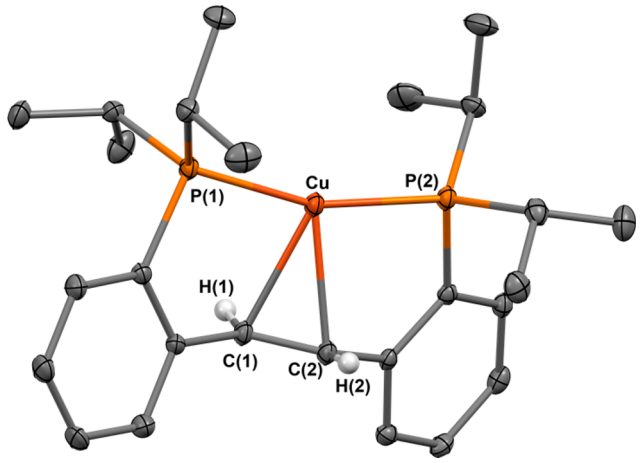

Figure 11. Thermal-ellipsoid (50% probability level) representation of the cationic fragment of **11**. Most hydrogen atoms and the counterion were omitted for clarity. Selected distances (Å) and angles (deg): Cu—P(1) = 2.2123(8), Cu—P(2) = 2.2122(8), C(1)—C(2) = 1.340(4), Cu—C(1) = 2.340(3), Cu—C(2) = 2.337(3), P(1)—Cu—P(2) = 162.34(4).

distances of 2.340(3) and 2.337(3) Å are longer than those in previously observed copper olefin complexes, which show values around 2.0 Å.[65−67] Such long distances imply that the interaction between the metal center and the olefin is weak. This observation is supported by the lack of elongation of the olefin C—C bond (1.340(4) Å).

In order to understand the bonding situation in the cationic copper(I) complexes, coordinates starting with values obtained from the X-ray structure were optimized using DFT (Figure 12). Interestingly, the optimized structure indicates that the

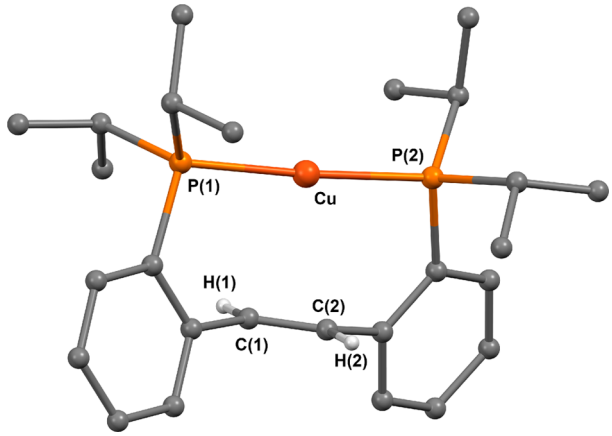

Figure 12. Optimized geometry for [(*t*PCH═CHP)Cu]$^+$. Most hydrogen atoms were removed for clarity. Selected distances (Å) and angles (deg): Cu—P(1) = 2.316, Cu—P(2) = 2.316, C(1)—C(2) = 1.360, Cu—C(1) = 2.704, Cu—C(2) = 2.712, P(1)—Cu—P(2) = 176.67.

olefin is not bound to copper and shows mild deviations from a linear geometry around the metal center, with a P(1)—Cu—P(2) angle of 176.67°. The distance from the olefin centroid to the metal center is 2.621 Å, compared to the value of 2.240 Å found crystallographically. These findings agree with a linear structure in which the olefin remains dissociated from the metal center. These results, coupled with the lack of evidence for olefin coordination in both ^{1}H and ^{13}C NMR spectra indicate

dx.doi.org/10.1021/ic500549z | *Inorg. Chem.* 2014, 53, 7248−7259

that the weakly bound olefin observed in the solid state structure dissociates in solution to generate a two-coordinate copper(I) complex.

The DFT results discussed above are also supported by the formation of the silver(I) complex [(*t*PCH═CHP)Ag][PF_6]

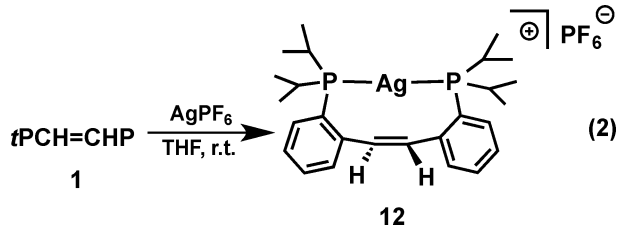

(2)

(**12**) that was observed upon mixing **1** with $AgPF_6$ (eq 2). The ^{1}H NMR spectrum of **12** shows one environment for the four methine protons, at 2.64 ppm, and two positions for the eight *iso*-propyl methyl groups at 1.27 and 1.10 ppm, respectively, indicating a symmetrical solution structure. Additionally, the olefinic protons appear as a singlet at 7.03 ppm, slightly upfield shifted from the corresponding values in the free ligand. The phosphines are found as a doublet at 29.62 ppm in the ^{31}P NMR spectrum. The broadness of the peaks is due to similar ^{107}Ag–^{31}P and ^{109}Ag–^{31}P coupling constants. The PF_6 counterion is found as a septet at −143.24 ppm in the ^{31}P NMR spectrum. Single crystals were obtained from a concentrated CH_2Cl_2 solution layered with *n*-pentane. The solid state molecular structure (Figure 13) indicates a nearly

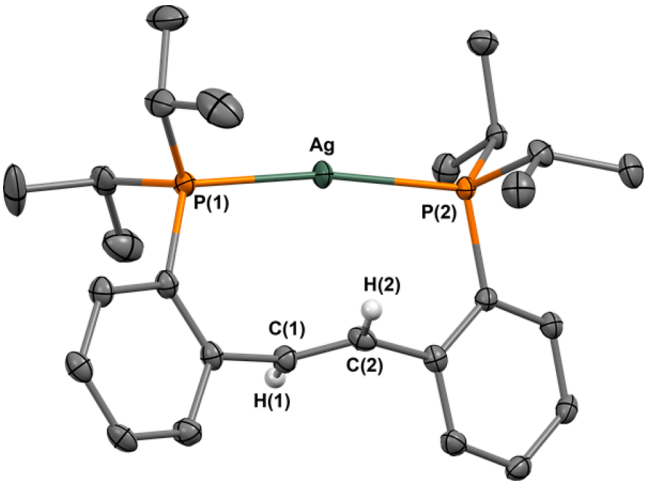

Figure 13. Thermal-ellipsoid (50% probability level) representation of the cationic fragment of **12**. Most hydrogen atoms and the counterion were omitted for clarity. Selected distances (Å) and angles (deg): Ag—P(1) = 2.3744(6), Ag—P(2) = 2.3789(6), C(1)—C(2) = 1.326(4), P(1)—Ag—P(2) = 168.32(2).

linear geometry around silver (P—Ag—P angle of 168.32(2)°), in which only the phosphines are coordinated to the metal center, unlike what was observed for the cationic copper(I) complex **11**. The difference between the two compounds is in agreement with the predominant preference of silver(I) to form dicoordinate complexes,[68−70] although in the absence of a better donating ligand, silver(I) can coordinate to olefinic moieties.[71] The Ag—P distances of 2.3744(6) and 2.3789(6) Å are similar to previously reported Ag—P distances.[69] The observed structure is reminiscent of [(2,6-bis[(di-*tert*-butylphosphino)methyl]pyridine)Ag][BF_4] containing a neutral ligand.[69] Compounds **12** and [(PNP)Ag][BF_4], however, are different from a silver(I) complex containing a monoanionic diaryl-amido based PNP ligand, [(PNP)Ag]$_2$ (PNP = bis(*o*-di-*iso*-propylphosphine-phenyl)amine), which leads to the formation of a dimeric species.[72] Using a similar ligand, Bourissou observed κ^2-P,P-coordination of $Ph_2P(C_6H_4)Me_2Si$-$SiMe_2(C_6H_4)PPh_2$ to silver(I), but a weak interaction between the Si—Si backbone and copper(I).[73]

CONCLUSIONS

The coordination chemistry of a neutral *t*PCH═CHP pincer with various first-row transition metals that form stable complexes in the +1 oxidation state was studied. In order to determine whether the coordination mode is dependent on the oxidation state of the metal, some +2 metal complexes were also synthesized and investigated. The backbone olefinic moiety is versatile and responds to the electronic requirements of the metal. When the metal center prefers a tetrahedral geometry (in (*t*PCH═CHP)$FeBr_2$ and (*t*PCH═CHP)$CoCl_2$) or linear geometry (in [(*t*PCH═CHP)Ag][PF_6]), the coordination of the C—C double bond is not observed; however, with low valent metal centers (in (*t*PCH═CHP)CoCl, (*t*PCH═CHP)-CoCl(CO), (*t*PCH═CHP)RhCl, and [(*t*PCH═CHP)Cu]-[PF_6]), η^2-coordination of the olefin occurs. Cobalt(II), iron(II), and copper(I) complexes presented an interesting case study since both noncoordination (in (*t*PCH═CHP)-$CoCl_2$, (*t*PCH═CHP)$FeBr_2$, and (*t*PCH═CHP)Cu(OTf)) and η^2-coordination (in [(*t*PCH═CHP)CoCl][$BAr^F{}_4$], [(*t*PCH═CHP)FeBr][$BAr^F{}_4$], and [(*t*PCH═CHP)Cu][PF_6]) of the olefinic backbone were observed. In square-planar complexes, [(*t*PCH═CHP)CoCl][$BAr^F{}_4$], (*t*PCH═CHP)-CoCl, and (*t*PCH═CHP)RhCl, the olefin tends to approach a perpendicular orientation with respect to the plane of the other ligands, while a T-shape geometry (in [(*t*PCH═CHP)Cu][PF_6]) prevents the olefin from rotating out of the plane.

The strength of the interaction between the olefin and the metal center was determined by NMR spectroscopy and X-ray crystallography (Table 1). The olefin peaks for free ligand are found downfield at 8.52 ppm in the ^{1}H NMR spectrum and 132.67 ppm in the corresponding ^{13}C NMR spectrum. As the olefin interacts with the metal center, the resulting shielding can significantly shift these peaks upfield, consistent with a reduction in the double bond character. This interaction is demonstrated in the cobalt(I) and rhodium(I) complexes **6**–**8** (Table 1). Similarly, the strength of the interaction can be evaluated in the solid state by examining the olefinic C—C distance determined by X-ray crystallography. Complexes with more electron rich metal centers (cobalt(I), (*t*PCH═CHP)-CoCl, and rhodium(I), (*t*PCH═CHP)RhCl) contain the most elongated C—C distance in the olefinic backbone. As the metal center becomes more electron deficient, this effect begins to diminish. Intuitively, complexes lacking coordination of the olefin, (*t*PCH═CHP)$CoCl_2$ and (*t*PCH═CHP)$FeBr_2$, contain short C—C distances. It can also be concluded that metal–olefin interactions in group 11 metal complexes are weak. These complexes show olefin shifts above 7 ppm in the ^{1}H NMR spectra and 132 ppm in the corresponding ^{13}C NMR spectra. Similarly, the solid state molecular structures for these complexes lack the characteristics of a bound olefin. The cationic copper(I) complex [(*t*PCH═CHP)Cu][PF_6] provides the best evidence for an olefin–metal interaction, displaying a

dx.doi.org/10.1021/ic500549z | Inorg. Chem. 2014, 53, 7248−7259

Table 1. Comparison of Olefinic Parameters for Discussed Compounds[a]

compd	olefin ^{1}H shift (ppm)	olefin ^{13}C shift (ppm)	olefin C—C distance (Å)	M—centroid distance (Å)
*t*PCH=CHP (**1**)[b]	8.52	132.67	1.330(4)	
(*t*PCH=CHP)$CoCl_2$ (**2**)			1.317(8)	3.501
(*t*PCH=CHP)$FeBr_2$ (**3**)[b]			1.320(6)	3.596
[(*t*PCH=CHP)CoCl][BAr^F_4] (**4**)			1.397(6)	2.068
[(*t*PCH=CHP)FeBr][BAr^F_4] (**5**)[b]			1.332(14)	2.206
(*t*PCH=CHP)CoCl (**6**)[b]	2.01	53.89	1.442(5)	1.868
(*t*PCH=CHP)CoCl(CO) (**7**)	3.64, 4.68	70.28, 72.75	1.438(7)	1.901
(*t*PCH=CHP)RhCl (**8**)[b]	3.74	70.78	1.432(8)	1.964
(*t*PCH=CHP)CuI (**9**)	7.03	132.00		
(*t*PCH=CHP)CuOTf (**10**)[b]	7.19	132.61	1.294(5)	2.426
[(*t*PCH=CHP)Cu][PF_6] (**11**)	7.02	135.20	1.340(4)	2.240
optimized [(*t*PCH=CHP)Cu]$^+$			1.360	2.621
[(*t*PCH=CHP)Ag][PF_6] (**12**)	7.02	137.71	1.326(4)	2.860

[a]NMR spectra were recorded in $CDCl_3$. [b]C_6D_6 was used as the NMR solvent.

small elongation of the C—C distance, similar to the distance observed in the cationic iron(II) species [(*t*PCH=CHP)FeBr][BAr^F_4]. The conflicting nature of the NMR spectroscopic and crystallographic data for this complex was explained by the existence of different solution and the solid state structures.

The various coordination modes observed showed that *t*PCH=CHP is a versatile ligand and could accommodate different geometries enabling new reactivity behavior for specific metal centers. Especially encouraging is the hemilabile behavior observed for cobalt(II), iron(II), and copper(I) examples, and these complexes form the focus of our future studies.

EXPERIMENTAL SECTION

All manipulations of air and water sensitive compounds were performed under a dry nitrogen atmosphere using an MBraun drybox. Glassware, vials, and stirring bars were dried in an oven at 120 °C overnight and evacuated for 24 h in the antechamber before being brought into the drybox. All solvents were dried by passing through a column of activated alumina, followed by storage over molecular sieves and sodium. Deuterated solvents were purchased from Cambridge Isotope Laboratories. C_6D_6 was dried by stirring over CaH_2 followed by filtration. $CDCl_3$ was dried over molecular sieves. Compound *t*PCH=CHP (**1**) was synthesized according to the previously reported method.[32] All other chemicals were commercially available and used as received. NMR spectra were obtained on Bruker 400 and Bruker 500 spectrometers at ambient temperature. Chemical shift values are reported in ppm relative to residual internal protonated solvent or to a tetramethylsilane standard while using $CDCl_3$ for ^{1}H and ^{13}C{^{1}H} experiments. Coupling constants are reported in Hz. Magnetic moments were determined by the Evans method[74−76] using capillaries containing trimethoxybenzene in either $CDCl_3$ or C_6D_6 as a reference, and trimethoxybenzene in the sample solution. IR spectrum was acquired on a FT/IR-6300 Jasco instrument. CHN analyses were performed on a CE-440 elemental analyzer, or by Midwest Microlab, LLC. *Gaussian 03* (revision D.02)[77] was used for all reported calculations. The B3LYP (DFT) method was used to carry out the geometry optimizations on model compounds specified in text using the LANL2DZ basis set. The validity of the true minima was checked by the absence of negative frequencies in the energy Hessian.

Synthesis of (*t*PCH=CHP)$CoCl_2$ (2). A solution of **1** (100 mg, 0.242 mmol) in 5 mL of THF was added to a suspension of $CoCl_2$ (31.6 mg, 0.242 mmol) in 2 mL of THF. The mixture was allowed to stir at room temperature for 1 h. The volatiles were removed under reduced pressure resulting in a green residue of **2**. Trituration with 3−5 mL of *n*-pentane produced a teal powder (93.8 mg, 0.174 mmol, 71%). The teal powder was then dissolved in a minimum amount of THF, and the solution was layered with *n*-pentane in order to obtain crystals suitable for X-ray diffraction. Magnetic moment: μ_{eff} = 3.34 μ_B. ^{1}H NMR (500 MHz, $CDCl_3$) δ: −0.59 ($\nu_{1/2}$ = 290.35 Hz, 12H, $CH(CH_3)_2$), 3.76 ($\nu_{1/2}$ = 286.53 Hz, 12H, $CH(CH_3)_2$), 6.35 ($\nu_{1/2}$ = 95.51 Hz, 4H, Ar*H*), 7.44 ($\nu_{1/2}$ = 133.71 Hz, 4H, ArH), 12.30 ($\nu_{1/2}$ = 175.74 Hz, 4 H, $CH(CH_3)_2$), 19.25 ($\nu_{1/2}$ = 443.16, 2H, C*H*=C*H*). Anal. Calcd for $C_{26}H_{38}Cl_2CoP_2$: C, 57.58; H, 7.06. Found: C, 57.50; H, 7.18.

Synthesis of (*t*PCH=CHP)$FeBr_2$ (3). A solution of **1** (100 mg, 0.242 mmol) in 5 mL of THF was added to a suspension of iron dibromide (52.1 mg, 0.241 mmol) in 2 mL of THF and allowed to stir at room temperature for 1 h. The volatiles were removed under reduced pressure resulting in a light brown residue of **3**. Trituration with 3−5 mL of *n*-pentane yielded a pure tan powder of **3** (126.3 mg, 0.201 mmol, 83%). Crystals suitable for single crystal X-ray diffraction were obtained through recrystallization from a concentrated solution of diethyl ether. Magnetic moment: μ_{eff} = 4.48 μ_B. ^{1}H NMR (500 MHz, C_6D_6) δ: 0.11 ($\nu_{1/2}$ = 204.99 Hz, 6H, $CH(CH_3)_2$), 2.87 ($\nu_{1/2}$ = 107.62 Hz, 6H, $CH(CH_3)_2$), 5.30 ($\nu_{1/2}$ = 440.72 Hz, 12H, $CH(CH_3)_2$), 6.83 ($\nu_{1/2}$ = 491.97 Hz, 8H, Ar*H*), 11.66 ($\nu_{1/2}$ = 645.70 Hz, 4 H, $CH(CH_3)_2$), 19.25 ($\nu_{1/2}$ = 901.94 Hz, 2H, C*H*=C*H*). Anal. Calcd for $C_{26}H_{38}Br_2FeP_2{\cdot}CHCl_3$: C, 43.38; H, 5.26. Found: C, 42.33; H, 5.12.

Synthesis of [(*t*PCH=CHP)CoCl][BAr^F_4] (4). A toluene solution of (*t*PCH=CHP)$CoCl_2$ (**2**, 20 mg, 0.04 mmol) was added to Na[BAr^F_4] (32.7 mg, 0.04 mmol). The mixture was stirred for 12 h until the solution turned from dark green to orange. The solution was filtered, followed by removal of the volatiles under reduced pressure leading to 36.6 mg, 71.8% of **4**. Compound **4** was recrystallized from a concentrated toluene solution layered with *n*-pentane chilled to −35 °C. Magnetic moment: μ_{eff} = 1.8 μ_B. ^{1}H NMR (500 MHz, $CDCl_3$) δ: −7.72 ($\nu_{1/2}$ = 503.7 Hz, 4H, $CH(CH_3)_2$), −3.4 ($\nu_{1/2}$ = 194.32 Hz, 12H, $CH(CH_3)_2$), −0.17 ($\nu_{1/2}$ = 503.70 Hz, 12H, $CH(CH_3)_2$), 3.25 ($\nu_{1/2}$ = 63.92 Hz, 2H, C*H*=C*H*), 6.16 ($\nu_{1/2}$ = 24.27 Hz, 2H, Ar*H*), 7.40 (4H, BArF-*H*), 7.57 (8H, BAr^F_4-*H*), 7.85 ($\nu_{1/2}$ =124.32 Hz, 2H, Ar*H*), 11.34 ($\nu_{1/2}$ = 957.28 Hz, 2H, Ar*H*), 15.17 ($\nu_{1/2}$ = 149.57, 2H, Ar*H*). ^{19}F NMR (470 MHz, $CDCl_3$) δ: −65.78 (BAr^F_4-*F*). ^{11}B NMR (160 MHz, $CDCl_3$) δ: −6.71(BAr^F_4). Anal. Calcd for $C_{58}H_{50}ClCoF_{24}P_2$: C, 50.84; H, 3.68. Found: C, 50.93; H, 3.56.

Synthesis of [(*t*PCH=CHP)FeBr][BAr^F_4] (5). To a solution of (*t*PCH=CHP)$FeBr_2$ (**3**, 25 mg, 0.40 mmol) in 5 mL of toluene was added a slurry of $NaBAr^F_4$ (35.4 mg, 0.40 mmol). The mixture was stirred for 12 h followed by removal of the volatiles under reduced pressure. The crude residue was triturated with *n*-pentane. Analytically pure **5** was obtained from a concentrated toluene solution layered with *n*-pentane at −35 °C (23.6 mg, 42.1%). μ_{eff} = 4.3 μ_B. ^{1}H NMR (400 MHz, C_6D_6) δ: 1.3 ($\nu_{1/2}$ = 166.45 Hz, 12H, $CH(CH_3)_2$), 5.43 ($\nu_{1/2}$ = 449.91 Hz, 12H, $CH(CH_3)_2$, 4H, $CH(CH_3)_2$), 7.51 (4H, BAr^F_4-*H*), 7.70 (8H, BAr^F_4-*H*), 9.82 ($\nu_{1/2}$ = 192.22 Hz, 2H, C*H*=C*H*), 10.95 ($\nu_{1/2}$ = 968.66 Hz, 4H, Ar*H*), 15.41 ($\nu_{1/2}$ = 116.84 Hz, 1H, Ar*H*),

dx.doi.org/10.1021/ic500549z | Inorg. Chem. 2014, 53, 7248−7259

17.86 ($\nu_{1/2}$ = 94.23 Hz, 1H, Ar*H*), 24.87 ($\nu_{1/2}$ = 242.23 Hz, 1H, Ar*H*), 26.51 ($\nu_{1/2}$ = 119.49 Hz, 1H, Ar*H*). ^{19}F NMR (376 MHz, C_6D_6) δ: −62.89 ($BAr^F{}_4$-*F*). ^{11}B NMR (128 MHz, C_6D_6) δ: −5.82 ($BAr^F{}_4$). Anal. Calcd for $C_{58}H_{50}BBrFeP_2F_{24}\cdot CH_2Cl_2$: C, 47.36; H, 3.50. Found: C, 47.01; H, 3.47.

Synthesis of (*t*PCH═CHP)CoCl (6). Complex **2** (75 mg, 0.138 mmol) was dissolved in 5 mL of THF. To this solution was added a suspension of 0.25 equiv of lithium aluminum hydride ($LiAlH_4$, 1.4 mg, 0.037 mmol). The resulting mixture was allowed to stir for 10 min at room temperature, after which it was filtered to give a purple solution. The volatiles were removed under reduced pressure producing a purple residue, which was dissolved in a minimum amount of *n*-pentane and allowed to crystallize at −35 °C (15.3 mg, 0.031 mmol, 22%). ^{1}H NMR (500 MHz, C_6D_6) δ: 1.00 (d, J_{PH} = 10 Hz, 6H, CH(C*H*$_3$)$_2$), 1.25 (d, J_{PH} = 5 Hz, 6H, CH(C*H*$_3$)$_2$), 1.37 (d, J_{PH} = 5 Hz, 6H, CH(C*H*$_3$)$_2$), 1.50 (d, J_{PH} = 10 Hz, 6H, CH(C*H*$_3$)$_2$), 2.01 (br s, 2H, C*H*═C*H*), 2.27 (br s, 2H, C*H*(CH$_3$)$_2$), 3.29 (br s, 2H, C*H*(CH$_3$)$_2$), 6.93 (t, J_{HH} = 5 Hz, 2H, Ar*H*), 6.97 (t, J_{HH} = 5 Hz, 2H, Ar*H*), 7.01 (d, J_{HH} = 10 Hz, 2H, Ar*H*), 7.14 (d, J_{HH} = 10 Hz, 2H, Ar*H*). ^{31}P{^{1}H} NMR (202 MHz, C_6D_6) δ: 58.11 (br s). ^{13}C{^{1}H} NMR (100 MHz, C_6D_6) δ: 16.34 (s, CH(*C*H$_3$)$_2$), 18.37 (s, CH(*C*H$_3$)$_2$), 20.15 (s, CH(*C*H$_3$)$_2$), 20.32 (s, CH(*C*H$_3$)$_2$), 22.88 (br s, *C*H(CH$_3$)$_2$), 24.18 (br s, *C*H(CH$_3$)$_2$), 53.89 (br s, *C*H═*C*H), 124.17 (s, Ar*C*), 125.12 (s, Ar*C*), 125.23 (s, Ar*C*), 129.38 (s, Ar*C*), 130.36 (s, Ar*C*),160.98 (s, Ar*C*). Anal. Calcd for $C_{26}H_{38}ClCoP_2$: C, 61.60; H, 7.56. Found: C, 61.58; H, 7.43.

Synthesis of (*t*PCH═CHP)CoCl(CO) (7). A THF solution of (*t*PCH═CHP)CoCl (**6**, 20 mg, 0.04 mmol) was added to a septum-capped vial along with a stir bar. The solution was then taken out of the glovebox, and CO was bubbled through the reaction mixture for 5 min. The starting deep purple solution rapidly turned bright orange. The reaction mixture was stirred for 1 h, and the volatiles were removed under reduced pressure. The crude reaction mixture was then dissolved in diethyl ether, filtered, and allowed to sit in a −35 °C freezer yielding crystals of **7** (11.9 mg, 0.02 mmol, 56.4%). ^{1}H NMR (400 MHz, C_6D_6) δ: 0.90 (dd, J_{PH} = 12 Hz, J_{HH} = 4 Hz, 3 H, CH(C*H*$_3$)$_2$), 1.04 (dd, J_{PH} = 12 Hz, J_{HH} = 4 Hz, 3H, CH(C*H*$_3$)$_2$), 1.23 (m, 6H, CH(C*H*$_3$)$_2$), 1.50 (m, 12H, CH(C*H*$_3$)$_2$), 2.24 (m, 2H, C*H*(CH$_3$)$_2$), 2.68 (m, 2H, C*H*(CH$_3$)$_2$), 2.92 (m, 1H, C*H*(CH$_3$)$_2$), 3.64 (m, 1H, C*H*═C*H*), 4.68 (m, 1H, C*H*═C*H*), 6.94 (m, 6H, Ar*H*), 7.08 (t, J_{HH} = 5 Hz, Ar*H*), 7.32 (d, J_{HH} = 8 Hz, Ar*H*). ^{31}P NMR (162 MHz, C_6D_6) δ: 71.96 (d, J_{PP} = 172 Hz), 75.05 (d, J_{PP} = 175 Hz). ^{13}C NMR (100 MHz, C_6D_6) δ: 18.12 (d, J_{CP} = 4 Hz, CH(CH$_3$)$_2$), 18.17 (s, CH(*C*H$_3$)$_2$), 18.60 (s, CH(*C*H$_3$)$_2$), 18.82 (d, J_{CP} = 5 Hz, CH(CH$_3$)$_2$), 20.08 (d, J_{PC} = 2 Hz, CH(CH$_3$)$_2$), 20.15 (s, CH(*C*H$_3$)$_2$), 20.31 (s, CH(*C*H$_3$)$_2$), 21.18 (s, CH(*C*H$_3$)$_2$), 26.28 (d, J_{CP} = 2 Hz, CH(CH$_3$)$_2$), 26.51 (d, J_{CP} = 2 Hz, *C*H(CH$_3$)$_2$), 26.70 (d, J_{CP} = 3 Hz, CH(CH$_3$)$_2$), 26.94 (d, J_{CP} = 3 Hz, *C*H(CH$_3$)$_2$), 26.99 (d, J_{CP} = 3 Hz, CH(CH$_3$)$_2$), 26.18 (d, J_{CP} = 2 Hz, CH(CH$_3$)$_2$), 28.04 (d, J_{CP} = 2 Hz, CH(CH$_3$)$_2$), 28.23 (d, J_{CP} = 2 Hz, CH(CH$_3$)$_2$), 70.28 (d, J_{CP} = 5 Hz, *C*H═CH), 72.75 (d, J_{CP} = 6 Hz, *C*H═CH), 125.13 (d, J_{CP} = 5 Hz, Ar*C*), 125.53 (d, J_{CP} = 4 Hz, Ar*C*), 126.15 (s, Ar*C*), 126.26 (s, Ar*C*), 126.91 (d, J_{CP} = 29 Hz, Ar*C*), 127.24 (d, J_{PC} = 30 Hz, Ar*C*), 127.10 (s, Ar*C*), 130.23 (d, J_{CP} = 3 Hz, Ar*C*), 130.46 (d, J_{CP} = 3 Hz, Ar*C*), 131.64 (s, Ar*C*), 131.96 (s, Ar*C*), 158.78 (dd, J_{PC} = 26 Hz, J_{PC} = 5 Hz, Ar*C*), 159.65 (dd, J_{PC} = 26 Hz, J_{PC} = 5 Hz, Ar*C*), 204.93 (br s, CO). IR (ATR) ν_{CO} = 1942 (s) cm^{-1}. Anal. Calcd for $C_{27}H_{38}ClCoOP_2$: C, 60.62; H, 7.16. Found: C, 60.39; H, 7.05.

Synthesis of (*t*PCH═CHP)RhCl (8). A mixture of *t*PCH═CHP (**1**, 25.0 mg, 0.061 mmol) and rhodium cyclooctadiene dichloride dimer ([(cod)RhCl]$_2$, 14.9 mg, 0.030 mmol) in THF was allowed to stir at room temperature for 1 h. The volatiles were removed under reduced pressure and the remaining yellow residue dissolved in *n*-pentane. The solution was placed in a −34 °C freezer, and crystals were obtained (23.0 mg, 0.0418 mmol, 69%). ^{1}H NMR (500 MHz, C_6D_6) δ: 1.00 (dd, J_{PH} = 13 Hz, J_{HH} = 6 Hz, 6H, CH(C*H*$_3$)$_2$), 1.12 (dd, J_{PH} = 16 Hz, J_{HH} = 8 Hz, 6H, CH(C*H*$_3$)$_2$), 1.22 (dd, J_{PH} = 16 Hz, J_{HH} = 8 Hz, 6 H, CH(C*H*$_3$)$_2$), 1.55 (dd, J_{PH} = 16 Hz, J_{HH} = 8 Hz, 6H, CH(C*H*$_3$)$_2$), 2.22 (br m, 2H, C*H*(CH$_3$)$_2$), 3.24 (m, 2H, C*H*(CH$_3$)$_2$), 3.74 (br d, J_{RhH} = 5 Hz, 2H, C*H*═C*H*), 7.00 (m, 4H, Ar*H*), 7.09 (br d, J_{HH} = 10 Hz, 4H, Ar*H*). ^{31}P{^{1}H} NMR (202 MHz, C_6D_6) δ: 57.10 (d, J_{RhP} = 120 Hz). ^{13}C{^{1}H} NMR (100 MHz, C_6D_6) δ: 16.89 (s, CH(*C*H$_3$)$_2$), 18.52 (t, $J_{PC} \sim J_{RhC}$ = 3 Hz, CH(*C*H$_3$)$_2$), 20.49 (t, $J_{PC} \sim J_{RhC}$ = 3 Hz, CH(*C*H$_3$)$_2$), 20.62 (t, $J_{PC} \sim J_{RhC}$ = 4 Hz, CH(*C*H$_3$)$_2$), 24.09 (m, CH(*C*H$_3$)$_2$), 70.78 (d, J_{RhC} = 17 Hz, *C*H═*C*H), 126.60 (t, J_{PC} = 3 Hz, Ar*C*), 126.25 (td, J_{PC} = 16 Hz, J_{RhC} = 3 Hz, Ar*C*), 127.71 (td, J_{RhC} = 1 Hz, J_{PC} = 7 Hz, Ar*C*), 130.29 (s, Ar*C*), 131.41 (s, Ar*C*), 158.08 (t, J_{PC} = 6 Hz, Ar*C*). Anal. Calcd for $C_{26}H_{38}ClRhP_2\cdot C_4H_{10}O$: C, 57.65; H, 7.74. Found: C, 57.81; H, 7.61.

Synthesis of (*t*PCH═CHP)CuI (9). Copper iodide (23.0 mg, 0.121 mmol) was mixed with *t*PCH═CHP (**1**, 50 mg, 0.121 mmol) in THF and stirred for 1 h at room temperature. The volatiles were removed under reduced pressure, and the resulting residue was triturated with *n*-pentane (67.8 mg, 0.113 mmol, 93%). ^{1}H NMR (500 MHz, $CDCl_3$) δ: 1.25 (app q, $J_{PH} \sim J_{HH}$ = 5 Hz, 6H, CH(C*H*$_3$)$_2$), 1.35 (app q, $J_{PH} \sim J_{HH}$ = 5 Hz, 6H, CH(C*H*$_3$)$_2$), 2.50 (m, 4H, C*H*(CH$_3$)$_2$), 7.03 (s, 2H, C*H*═C*H*), 7.33 (m, 4H, Ar*H*), 7.35 (m, 2H, Ar*H*), 7.40 (app t, J_{HH} = 10 Hz, 2H, Ar*H*), 7.53 (m, 2H, Ar*H*). ^{31}P{^{1}H} NMR (202 MHz, $CDCl_3$) δ: 7.00 (br s). ^{13}C{^{1}H} NMR (126 MHz, $CDCl_3$) δ: 19.91 (t, J_{PC} = 3.78, CH(*C*H$_3$)$_2$), 20.58 (br t, J_{PC} = 1.26 Hz, CH(*C*H$_3$)$_2$), 25.88 (t, J_{PC} = 7.56 Hz, *C*H(CH$_3$)$_3$), 127.41 (s, Ar*C*), 129.43 (t, J_{PC} = 3.78 Hz, Ar*C*), 129.98 (s, Ar*C*), 132.00 (t, J_{PC} = 6.30 Hz, *C*H═CH), 132.58 (s, Ar*C*), 132.86 (t, J_{PC} = 15 Hz, Ar*C*), 145.71 (t, J_{PC} = 11.34 Hz, Ar*C*). Anal. Calcd for $C_{26}H_{38}CuIP_2$: C, 51.79; H, 6.35. Found: C 52.40; H 6.18.

Synthesis of (*t*PCH═CHP)CuOTf (10). Compound **9** (33.9 mg, 0.056 mmol) was dissolved in THF and added to silver triflate (14.4 mg, 0.056 mmol). The mixture was stirred at room temperature for 1 h. The solution was then filtered, followed by removal of the volatiles under reduced pressure. The resulting crude oil was triturated with *n*-pentane leading to a white powder (33.4 mg, 0.053 mmol, 95%). The powder was recrystallized from a toluene solution layered with *n*-pentane at −35 °C. ^{1}H NMR (500 MHz, C_6D_6) δ: 1.01 (app q, J_{PH} = 10 Hz, J_{HH} = 5 Hz, 12 H, CH(C*H*$_3$)$_2$), 1.10 (app q, J_{PH} = 10 Hz, J_{HH} = 5 Hz, 12H, CH(C*H*$_3$)$_2$), 2.14 (m, 4H, C*H*(CH$_3$)$_2$), 7.09 (m, 2H, Ar*H*), 7.19 (m, 8 H, Ar*H*, C*H*═C*H*). ^{31}P{^{1}H} NMR (202 MHz, C_6D_6) δ: 14.54 (s) ^{19}F{^{1}H} NMR (470 MHz, C_6D_6) δ: 80.82 (s, C*F*$_3$). ^{13}C{^{1}H} NMR (126 MHz, C_6D_6) δ: 19.74 (t, J_{PC} = 4 Hz, CH(CH$_3$)$_2$), 19.97 (br s, CH(*C*H$_3$)$_2$), 24.64 (t, J_{PC} = 9 Hz, CH(CH$_3$)$_2$), 127.77 (s, Ar*C*), 129.68 (t, J_{PC} = 4 Hz, Ar*C*), 130.59 (s, Ar*C*), 132.19 (s, Ar*C*), 132.61 (br t, J_{PC} = 6 Hz, *C*H═*C*H), 133.09 (t, J_{PH} = 18 Hz, Ar*C*), 146.24 (t, J_{PC} = 11 Hz, Ar*C*). Anal. Calcd for $C_{26}H_{38}CuF_6P_3$: C, 50.28; H, 6.17. Found: C 50.23; H 6.12.

Synthesis of [(*t*PCH═CHP)Cu][PF$_6$] (11). A solution of (*t*PC═CP)CuI (**9**, 52.5 mg, 0.12 mmol) in THF was added to a slurry of $AgPF_6$ (30.8 mg, 0.12 mmol), and stirred at room temperature for 1 h. The volatiles were removed under reduced pressure, followed by trituration with *n*-pentane that resulted in a white powder (46.3 mg, 0.10 mmol, 84.6%). ^{1}H NMR (400 MHz, $CDCl_3$) δ: 1.11 (q, $J_{PH} \sim J_{HH}$ = 8 Hz, 12 H, CH(C*H*$_3$)$_2$), 1.27 (q, $J_{PH} \sim J_{HH}$ = 8 Hz, 12 H, CH(C*H*$_3$)$_2$), 2.62 (m, 4H, C*H*(H$_3$)$_2$), 7.02 (s, 2H, C*H*═C*H*), 7.60 (m, 8 H, Ar*H*). ^{31}P{^{1}H} NMR (162 MHz, $CDCl_3$) δ: −143.28 (septet, J_{PF} = 708 Hz, *P*F$_6$), 25.41 (s, *P*^{i}Pr$_2$). ^{19}F {^{1}H} NMR (376 MHz, $CDCl_3$) δ: −76.63 (d, J_{FP} = 711 Hz, PF$_6$). ^{13}C{^{1}H} NMR (100 MHz, $CDCl_3$) δ: 19.03 (s, CH(*C*H$_3$)$_2$), 20.17 (t, J_{CP} = 4 Hz, CH(*C*H$_3$)$_2$), 23.55 (t, J_{CP} = 11 Hz, *C*H(CH$_3$)$_2$), 129.37 (s, Ar*C*), 129.86 (s, Ar*C*), 129.91 (s, Ar*C*), 132.37 (s, Ar*C*), 133.11 (s, Ar*C*), 135.20 (br s, *C*H═*C*H), 144.68 (t, J_{CP} = 11 Hz, Ar*C*). Anal. Calcd for $C_{27}H_{38}CuF_3O_3P_2S$: C, 51.88; H, 6.13. Found: C 51.79; H 6.12.

Synthesis of [(*t*PCH═CHP)Ag][PF$_6$] (12). A THF solution of *t*PCH═CHP (**1**, 25 mg, 0.061 mmol) was mixed with a suspension of $AgPF_6$ (15.4 mg, 0.061 mmol) and stirred at ambient temperature for 1 h. The volatiles were then removed under reduced pressure, followed by trituration of the crude residue with pentanes, resulting in a white powder of [(*t*PCH═CHP)Ag][PF$_6$] (38.7 mg, 0.057 mmol, 96%). The product was then recrystallized from a concentrated CH_2Cl_2 solution layered with *n*-pentane. ^{1}H NMR (400 MHz, $CDCl_3$) δ: 1.18 (app q, J_{ph} = 8 Hz, 12H, CH(C*H*$_3$)$_2$), 1.29 (m, 12H, CH(C*H*$_3$)$_2$), 2.65 (m, 4H, C*H*(CH$_3$)$_2$), 7.03 (br s, 2H, C*H*═C*H*), 7.51 (m, 2 H, Ar*H*), 7.74 (d, J_{HH} = 4 Hz, 2 H, Ar*H*), 7.61 (m, 4 H, Ar*H*). ^{31}P{^{1}H} NMR

dx.doi.org/10.1021/ic500549z | Inorg. Chem. 2014, 53, 7248−7259

(162 MHz, $CDCl_3$) δ: −143.24 (septet, J_{PF} = 714.4 Hz, PF_6), 29.62 (d, unresolved ^{107}Ag−P, ^{109}Ag−P coupling, Ar-P^iPr_2). $^{19}F\{^1H\}$ NMR (376 MHz, $CDCl_3$) δ: −76.18 (d, J_{PF} = 718.2 Hz, PF_6). $^{13}C\{^1H\}$ NMR (100 MHz, $CDCl_3$) δ: 18.81 (s, $CH(CH_3)_2$), 20.19 (t, J_{CP} = 5 Hz, $CH(CH_3)_2$, 23.87 (t, J_{PC} = 10 Hz, $CH(CH_3)_2$), 126.05 (t, J_{PC} = 17 Hz, ArC), 128.68 (t, J_{PC} = 3 Hz, ArC), 130.87 (s, ArC), 131.80 (s, ArC), 133.28 (s, ArC), 137.71 (br s, CH═CH), 144.49 (t, J_{PC} = 9 Hz, ArC). Anal. Calcd for $C_{26}H_{38}AgF_6P_3$: C, 46.93, H, 5.76. Found: C 46.84, H 5.77.

X-ray Crystal Structure of (*t*PCH═CHP)$CoCl_2$ (2). X-ray quality single crystals were obtained from a concentrated CH_2Cl_2 solution layered with *n*-pentane at −35 °C in the glovebox. Crystal and refinement data for **2**: $C_{26}H_{38}Cl_2CoP_2$; M_r = 542.33; monoclinic; space group *Cc*; *a* = 18.254(2) Å; *b* = 18.645(2) Å; *c* = 16.109(2) Å; α = 90°; β = 97.618(3)°; γ = 90°; *V* = 5434.2(12) Å^3; *Z* = 8; *T* = 120(2) K; λ = 0.710 73 Å; μ = 0.958 mm^{-1}; d_{calc} = 1.326 g cm^{-3}; 35 511 reflections collected; 11 030 unique (R_{int} = 0.1341); giving R1 = 0.0583, wR2 = 0.0652 for 6488 data with $[I > 2\sigma(I)]$ and R1 = 0.1370, wR2 = 0.0819 for all 11 030 data. Residual electron density (e$^-$ Å^{-3}) max/min: 0.460/−0.508.

X-ray Crystal Structure of (*t*PCH═CHP)$FeBr_2$ (3). X-ray quality single crystals were obtained from a concentrated solution of diethyl ether at −35 °C in the glovebox as pale yellow rods. Crystal and refinement data for **3**: $C_{26}H_{38}Br_2FeP_2$; M_r = 628.17; monoclinic; space group $P2_1/n$; *a* = 15.9893(19) Å; *b* = 11.1028(13) Å; *c* = 16.3823(19) Å; α = 90°; β = 107.936(2)°; γ = 90°; *V* = 2766.9(6) Å^3; *Z* = 4; *T* = 120(2) K; λ = 0.710 73 Å; μ = 3.561 mm^{-1}; d_{calc} = 1.508 g cm^{-3}; 26 462 reflections collected; 5729 unique (R_{int} = 0.0880); giving R1 = 0.0445, wR2 = 0.0973 for 4035 data with $[I > 2\sigma(I)]$ and R1 = 0.0799, wR2 = 0.1068 for all 5729 data. Residual electron density (e$^-$ Å^{-3}) max/min: 0.780/−0.967.

X-ray Crystal Structure of [(*t*PCH═CHP)CoCl][BAr^F_4] (4). X-ray quality single crystals were obtained from a concentrated toluene solution layered with *n*-pentane at −35 °C in the glovebox. Crystal and refinement data for **4**: $C_{129}H_{108}B_2Cl_2Co_2F_{48}P_4$; M_r = 2904.41; triclinic; space group $P\bar{1}$; *a* = 12.4634(16) Å; *b* = 23.274(3) Å; *c* = 24.594(3) Å; α = 74.884(3)°; β = 77.262(3)°; γ = 78.423(3)°; *V* = 6639.6(15) Å^3; *Z* = 2; *T* = 120(2) K; λ = 0.710 73 Å; μ = 0.453 mm^{-1}; d_{calc} = 1.453 g cm^{-3}; 154 657 reflections collected; 23 349 unique (R_{int} = 0.0586); giving R1 = 0.0711, wR2 = 0.1898 for 17 148 data with $[I > 2\sigma(I)]$ and R1 = 0.0983, wR2 = 0.2049 for all 23 349 data. Residual electron density (e$^-$ Å^{-3}) max/min: 1.779/−1.155.

X-ray Crystal Structure of [(*t*PCH═CHP)FeBr][BAr^F_4] (5). X-ray quality single crystals were obtained from a concentrated toluene solution layered with *n*-pentane at −35 °C in the glovebox. Crystal and refinement data for **5**: $C_{65}H_{58}BBrF_{24}FeP_2$; M_r = 1503.62; triclinic; space group $P\bar{1}$; *a* = 13.1231(6) Å; *b* = 13.6718(7) Å; *c* = 18.7070(9) Å; α = 79.3172(19)°; β = 80.9439(19)°; γ = 86.7229(19)°; *V* = 3255.7(3) Å^3; *Z* = 2; *T* = 120(2) K; λ = 0.710 73 Å; μ = 1.004 mm^{-1}; d_{calc} = 1.534 g cm^{-3}; 71 334 reflections collected; 11 462 unique (R_{int} = 0.0262); giving R1 = 0.0407, wR2 = 0.1049 for 9966 data with $[I > 2\sigma(I)]$ and R1 = 0.0485, wR2 = 0.1090 for all 11 462 data. Residual electron density (e$^-$ Å^{-3}) max/min: 1.490/−1.684.

X-ray Crystal Structure of (*t*PCH═CHP)CoCl (6). X-ray quality single crystals were obtained from a concentrated THF solution layered with *n*-pentane in a −35 °C freezer in the glovebox as dark purple blocks. Crystal and refinement data for **6**: $C_{26}H_{38}ClCoP_2$; M_r = 506.88; monoclinic; space group $P2_1/c$; *a* = 11.011(2) Å; *b* = 7.7640(14) Å; *c* = 29.925(6) Å; α = 90°; β = 90.224(4)°; γ = 90°; *V* = 2558.3(8) Å^3; *Z* = 4; *T* = 120(2) K; λ = 0.710 73 Å; μ = 0.912 mm^{-1}; d_{calc} = 1.316 g cm^{-3}; 23 379 reflections collected; 5325 unique (R_{int} = 0.0579); giving R1 = 0.0474, wR2 = 0.1050 for 4386 data with $[I > 2\sigma(I)]$ and R1 = 0.0574, wR2 = 0.1078 for all 5325 data. Residual electron density (e$^-$ Å^{-3}) max/min: 0.360/−0.569.

X-ray Crystal Structure of (*t*PCH═CHP)CoCl(CO) (7). X-ray quality single crystals were obtained from a concentrated diethyl ether solution in a −35 °C freezer in the glovebox. Crystal and refinement data for **7**: $C_{27}H_{38}ClCoOP_2$; M_r = 534.89; orthorhombic; space group *Pbca*; *a* = 9.9988(6) Å; *b* = 15.4852(10) Å; *c* = 34.356(2) Å; α = 90°; β = 90°; γ = 90°; *V* = 5319.4(6) Å^3; *Z* = 8; *T* = 120(2) K; λ = 0.71073 Å; μ = 0.884 mm^{-1}; d_{calc} = 1.336 g cm^{-3}; 72 798 reflections collected; 4673 unique (R_{int} = 0.1264); giving R1 = 0.0824, wR2 = 0.1280 for 3927 data with $[I > 2\sigma(I)]$ and R1 = 0.1028, wR2 = 0.1333 for all 4673 data. Residual electron density (e$^-$ Å^{-3}) max/min: 0.639/−0.739.

X-ray Crystal Structure of (*t*PCH═CHP)RhCl (8). X-ray quality single crystals were obtained as yellow plates from a concentrated diethyl ether solution at −35 °C in the glovebox. Crystal and refinement data for **8**: $C_{26}H_{38}ClP_2Rh$; M_r = 550.86; monoclinic; space group *P*2/*c*; *a* = 11.8111(12) Å; *b* = 15.7865(16) Å; *c* = 14.7769(15) Å; α = 90°; β = 110.3090(17)°; γ = 90°; *V* = 2584.0(5) Å^3; *Z* = 4; *T* = 120(2) K; λ = 0.710 73 Å; μ = 0.900 mm^{-1}; d_{calc} = 1.416 g cm^{-3}; 33 562 reflections collected; 5298 unique (R_{int} = 0.0847); giving R1 = 0.0627, wR2 = 0.0906 for 4019 data with $[I > 2\sigma(I)]$ and R1 = 0.0893, wR2 = 0.0958 for all 5298 data. Residual electron density (e$^-$ Å^{-3}) max/min: 1.349/−1.619.

X-ray Crystal Strucure of (*t*PCH═CHP)Cu(OTf) (10). X-ray quality single crystals were obtained as clear blocks from a toluene solution layered with *n*-pentane at −35 °C in the glovebox. Crystal and refinement data for **10**: formula $C_{27}H_{38}CuF_3O_3P_2S$; M_r = 625.11; orthorhombic; space group *Pbca*; *a* = 10.2443(8) Å; *b* = 18.9199(15) Å; *c* = 30.626(3) Å; α = 90°; β = 90°; γ = 90°; *V* = 5936.0(8) Å^3; *Z* = 8; *T* = 120(2) K; λ = 0.710 73 Å; μ = 0.959 mm^{-1}; d_{calc} = 1.399 g cm^{-3}; 119 904 reflections collected; 5232 unique (R_{int} = 0.0628); giving R1 = 0.0379, wR2 = 0.0910 for 4447 data with $[I > 2\sigma(I)]$ and R1 = 0.0476, wR2 = 0.0982 for all 5232 data. Residual electron density (e$^-$ Å^{-3}) max/min: 1.473/−0.541.

X-ray Crystal Strucure of [(*t*PCH═CHP)Cu][PF_6] (11). X-ray quality single crystals were obtained as clear blocks from a CH_2Cl_2 solution layered with *n*-pentane at −35 °C in the glovebox. Crystal data for **11**: formula: $C_{26}H_{38}CuF_6P_3$; M_r = 621.01; monoclinic; space group $P2_1/c$; *a* = 9.5653(4) Å; *b* = 21.5479(9) Å; *c* = 14.6122(6) Å; α = 90°; β = 103.1306(16)°; γ = 90°;*V* = 2933.0(2) Å^3; *Z* = 4; *T* = 120(2) K; λ = 0.710 73 Å; μ = 0.960 mm^{-1}; d_{calc} = 1.406 g cm^{-3}; 43 314 reflections collected; 5146 unique (R_{int} = 0.0580); giving R1 = 0.0411, wR2 = 0.0869 for 4211 data with $[I > 2\sigma(I)]$ and R1 = 0.0559, wR2 = 0.0924 for all 5146 data. Residual electron density (e$^-$ Å^{-3}) max/min: 2.142/−1.079.

X-ray Crystal Strucure of [(*t*PCH═CHP)Ag][PF_6] (12). X-ray quality single crystals were obtained as clear blocks from a CH_2Cl_2 solution layered with *n*-pentane at −35 °C in the glovebox. Crystal and refinement data for **12**: formula $C_{26}H_{38}AgF_6P_3$; M_r = 665.34; orthorhombic; space group $P2_12_12_1$; *a* = 9.8584(6) Å; *b* = 12.6977(7) Å; *c* = 23.1548(13) Å; α = 90°; β = 90°; γ = 90°; *V* = 2898.5(3) Å^3; *Z* = 4; *T* = 120(2) K; λ = 0.710 73 Å; μ = 0.914 mm^{-1}; d_{calc} = 1.525 g cm^{-3}; 53 763 reflections collected; 7281 unique (R_{int} = 0.0390); giving R1 = 0.0271, wR2 = 0.0590 for 6793 data with $[I > 2\sigma(I)]$and R1 = 0.0313, wR2 = 0.0611 for all 7281 data. Residual electron density (e$^-$ Å^{-3}) max/min: 0.562/−0.481.

■ ASSOCIATED CONTENT

Ⓢ Supporting Information

NMR spectra for compounds **2**−**12**, IR spectrum for compound **7**, complete ref 77, computational details, a text file of the computed molecular Cartesian coordinates in a format for convenient visualization, crystallographic tables and details (CIF) for compounds **2**−**8**, **10**−**12**. This material is available free of charge via the Internet at http://pubs.acs.org.

■ AUTHOR INFORMATION

Corresponding Author

*E-mail: viluc@nd.edu.

Notes

The authors declare no competing financial interest.

■ ACKNOWLEDGMENTS

We thank Dr. Allen Oliver and Dominic C. Babbini for crystallographic assistance. This work was supported by the

University of Notre Dame and by Donors of the American Chemical Society Petroleum Research Fund (ACS PRF 53536-DNI3).

REFERENCES

(1) Clapham, S. E.; Hadzovic, A.; Morris, R. H. *Coord. Chem. Rev.* **2004**, *248*, 2201.
(2) van der Vlugt, J. I.; Reek, J. N. H. *Angew. Chem., Int. Ed.* **2009**, *48*, 8832.
(3) Gunanathan, C.; Milstein, D. *Acc. Chem. Res.* **2011**, *44*, 588.
(4) Burford, R. J.; Piers, W. E.; Parvez, M. *Organometallics* **2012**, *31*, 2949.
(5) Friedrich, A.; Drees, M.; Kass, M.; Herdtweck, E.; Schneider, S. *Inorg. Chem.* **2010**, *49*, 5482.
(6) He, T.; Tsvetkov, N. P.; Andino, J. G.; Gao, X. F.; Fullmer, B. C.; Caulton, K. G. *J. Am. Chem. Soc.* **2010**, *132*, 910.
(7) Grutzmacher, H. *Angew. Chem., Int. Ed.* **2008**, *47*, 1814.
(8) Jeffrey, J. C.; Rauchfuss, T. B. *Inorg. Chem.* **1979**, *18*, 2658.
(9) Braunstein, P.; Naud, F. *Angew. Chem., Int. Ed.* **2001**, *40*, 680.
(10) Davies, J. A.; Hartley, F. R. *Chem. Rev.* **1981**, *81*, 79.
(11) Slone, C. S.; Weinberger, D. A.; Mirkin, C. A. *Prog. Inorg. Chem.* **1999**, *48*, 233.
(12) Bader, A.; Lindner, E. *Coord. Chem. Rev.* **1991**, *108*, 27.
(13) Gunanathan, C.; Ben-David, Y.; Milstein, D. *Science* **2007**, *317*, 790.
(14) Deckers, P. J. W.; Hessen, B.; Teuben, J. H. *Angew. Chem., Int. Ed.* **2001**, *40*, 2516.
(15) Nandi, M.; Jin, J.; RajanBabu, T. V. *J. Am. Chem. Soc.* **1999**, *121*, 9899.
(16) Otten, E.; Meetsma, A.; Hessen, B. *J. Am. Chem. Soc.* **2007**, *129*, 10100.
(17) Milner, P. J.; Maimone, T. J.; Su, M.; Chen, J.; Müller, P.; Buchwald, S. L. *J. Am. Chem. Soc.* **2012**, *134*, 19922.
(18) Lindner, R.; van den Bosch, B.; Lutz, M.; Reek, J. N. H.; van der Vlugt, J. I. *Organometallics* **2011**, *30*, 499.
(19) Anderson, J. S.; Rittle, J.; Peters, J. C. *Nature* **2013**, *501*, 84.
(20) Lee, D. W.; Jensen, C. M.; Morales-Morales, D. *Organometallics* **2003**, *22*, 4744.
(21) Selander, N.; Szabo, K. J. *Chem. Rev.* **2011**, *111*, 2048.
(22) Benito-Garagorri, D.; Kirchner, K. *Acc. Chem. Res.* **2008**, *41*, 201.
(23) Vankoten, G. *Pure Appl. Chem.* **1989**, *61*, 1681.
(24) Jensen, C. M. *Chem. Commun.* **1999**, 2443.
(25) Ines, B.; SanMartin, R.; Moure, M. J.; Dominguez, E. *Adv. Synth. Catal.* **2009**, *351*, 2124.
(26) van der Vlugt, J. I.; Pidko, E. A.; Vogt, D.; Lutz, M.; Spek, A. L.; Meetsma, A. *Inorg. Chem.* **2008**, *47*, 4442.
(27) Bauer, R. C.; Gloaguen, Y.; Lutz, M.; Reek, J. N. H.; de Bruin, B.; van der Vlugt, J. I. *Dalton Trans.* **2011**, *40*, 8822.
(28) Kohl, S. W.; Weiner, L.; Schwartsburd, L.; Konstantinovski, L.; Shimon, L. J. W.; Ben-David, Y.; Iron, M. A.; Milstein, D. *Science* **2009**, *324*, 74.
(29) Bennett, M. A.; Johnson, R. N.; Tomkins, I. B. *J. Organomet. Chem.* **1976**, *118*, 205.
(30) Bennett, M. A.; Clark, P. W. *J. Organomet. Chem.* **1976**, *110*, 367.
(31) Bennett, M. A.; Corlett, S.; Robertson, G. B.; Steffen, W. L. *Aust. J. Chem.* **1980**, *33*, 1261.
(32) Barrett, B. J.; Iluc, V. M. *Organometallics* **2014**, *33*, 2565.
(33) Yang, F.; Zhou, Q.; Zhang, Y. Q.; Zeng, G.; Li, G. H.; Shi, Z.; Wang, B. W.; Feng, S. H. *Chem. Commun.* **2013**, *49*, 5289.
(34) Marlier, E. E.; Tereniak, S. J.; Ding, K. Y.; Mulliken, J. E.; Lu, C. C. *Inorg. Chem.* **2011**, *50*, 9290.
(35) Affo, W.; Ohmiya, H.; Fujioka, T.; Ikeda, Y.; Nakamura, T.; Yorimitsu, H.; Oshima, K.; Imamura, Y.; Mizuta, T.; Miyoshi, K. *J. Am. Chem. Soc.* **2006**, *128*, 8068.
(36) Sharma, R. K.; RajanBabu, T. V. *J. Am. Chem. Soc.* **2010**, *132*, 3295.
(37) Mizuta, T.; Imamura, Y.; Miyoshi, K.; Yorimitsu, H.; Oshima, K. *Organometallics* **2005**, *24*, 990.
(38) Hou, J. X.; Sun, W. H.; Zhang, S.; Ma, H. W.; Deng, Y.; Lu, X. M. *Organometallics* **2006**, *25*, 236.
(39) Wang, M.; Yu, X. M.; Shi, Z.; Qian, M. X.; Jin, K.; Chen, J. H.; He, R. *J. Organomet. Chem.* **2002**, *645*, 127.
(40) Dong, Q. C.; Rose, M. J.; Wong, W. Y.; Gray, H. B. *Inorg. Chem.* **2011**, *50*, 10213.
(41) Grutters, M. M. P.; van der Vlugt, J. I.; Pei, Y.; Mills, A. M.; Lutz, M.; Spek, A. L.; Müller, C.; Moberg, C.; Vogt, D. *Adv. Synth. Catal.* **2009**, *351*, 2199.
(42) Brescianipahor, N.; Calligaris, M.; Randaccio, L.; Marzilli, L. G. *Inorg. Chim. Acta* **1979**, *32*, 181.
(43) Chadwell, S. J.; Coles, S. J.; Edwards, P. G.; Hursthouse, M. B. *J. Chem. Soc., Dalton Trans.* **1995**, 3551.
(44) Deblon, S.; Liesum, L.; Harmer, J.; Schonberg, H.; Schweiger, A.; Grutzmacher, H. *Chem.—Eur. J.* **2002**, *8*, 601.
(45) Snyder, B. S.; Holm, R. H. *Inorg. Chem.* **1988**, *27*, 2339.
(46) Kornev, A. N.; Belina, N. V.; Sushev, V. V.; Fukin, G. K.; Baranov, E. V.; Kurskiy, Y. A.; Poddelskii, A. I.; Abakumov, G. A.; Lonnecke, P.; Hey-Hawkins, E. *Inorg. Chem.* **2009**, *48*, 5574.
(47) Fryzuk, M. D.; Leznoff, D. B.; Ma, E. S. F.; Rettig, S. J.; Young, V. G. *Organometallics* **1998**, *17*, 2313.
(48) Hawrelak, E. J.; Bernskoetter, W. H.; Lobkovsky, E.; Yee, G. T.; Bill, E.; Chirik, P. J. *Inorg. Chem.* **2005**, *44*, 3103.
(49) Meehan, P. R.; Alyea, E. C.; Shakya, R. P.; Ferguson, G. *Polyhedron* **1998**, *17*, 11.
(50) Rozenel, S. S.; Padilla, R.; Arnold, J. *Inorg. Chem.* **2013**, *52*, 11544.
(51) Hermes, A. R.; Girolami, G. S. *Organometallics* **1987**, *6*, 763.
(52) Sciarone, T. J. J.; Nijhuis, C. A.; Meetsma, A.; Hessen, B. *Organometallics* **2008**, *27*, 2058.
(53) Jové, F. A.; Pariya, C.; Scoblete, M.; Yap, G. P. A.; Theopold, K. H. *Chem.—Eur. J.* **2011**, *17*, 1310.
(54) Black, M.; Mais, R. H. B.; Owston, P. G. *Acta. Crystallogr., Sect. B* **1969**, *B 25*, 1753.
(55) Hartley, F. R. *Angew. Chem., Int. Ed. Engl.* **1972**, *11*, 596.
(56) Dodoff, N. I.; Lalia-Kantouri, M.; Gdaniec, M.; Czapik, A.; Vassilev, N. G.; Markova, L. S.; Apostolova, M. D. *J. Coord. Chem.* **2012**, *65*, 688.
(57) Klein, H. F.; Karsch, H. H. *Inorg. Chem.* **1975**, *14*, 473.
(58) Hayashi, Y.; Szalda, D. J.; Grills, D. C.; Hanson, J. C.; Huang, K. W.; Muckerman, J. T.; Fujita, E. *Polyhedron* **2013**, *58*, 106.
(59) Vigalok, A.; Milstein, D. *J. Am. Chem. Soc.* **1997**, *119*, 7873.
(60) Okamoto, K.; Omoto, Y.; Sano, H.; Ohe, K. *Dalton Trans.* **2012**, *41*, 10926.
(61) Vigalok, A.; Rybtchinski, B.; Shimon, L. J. W.; Ben-David, Y.; Milstein, D. *Organometallics* **1999**, *18*, 895.
(62) Feller, M.; Ben-Ari, E.; Gupta, T.; Shimon, L. J. W.; Leitus, G.; Diskin-Posner, Y.; Weiner, L.; Milstein, D. *Inorg. Chem.* **2007**, *46*, 10479.
(63) Jia, G. C.; Lee, H. M.; Williams, I. D. *Organometallics* **1996**, *15*, 4235.
(64) Kumar, S.; Mani, G.; Dutta, D.; Mishra, S. *Inorg. Chem.* **2014**, *53*, 700.
(65) Harmata, M.; Ghosh, S. K.; Barnes, C. L. *J. Supramol. Chem.* **2002**, *2*, 349.
(66) Masuda, H.; Yamamoto, N.; Taga, T.; Machida, K.; Kitagawa, S.; Munakata, M. *J. Organomet. Chem.* **1987**, *322*, 121.
(67) Thompson, J. S.; Harlow, R. L.; Whitney, J. F. *J. Am. Chem. Soc.* **1983**, *105*, 3522.
(68) Budagumpi, S.; Haque, R. A.; Salman, A. W.; Ghdhayeb, M. Z. *Inorg. Chim. Acta* **2012**, *392*, 61.
(69) van der Vlugt, J. I.; Siegler, M. A.; Janssen, M.; Vogt, D.; Spek, A. L. *Organometallics* **2009**, *28*, 7025.
(70) Carvajal, M. A.; Novoa, J. J.; Alvarez, S. *J. Am. Chem. Soc.* **2004**, *126*, 1465.
(71) Reisinger, A.; Trapp, N.; Knapp, C.; Himmel, D.; Breher, F.; Rüegger, H.; Krossing, I. *Chem.—Eur. J.* **2009**, *15*, 9505.

(72) DeMott, J. C.; Basuli, F.; Kilgore, U. J.; Foxman, B. M.; Huffman, J. C.; Ozerov, O. V.; Mindiola, D. J. *Inorg. Chem.* **2007**, *46*, 6271.
(73) Gualco, P.; Amgoune, A.; Miqueu, K.; Ladeira, S.; Bourissou, D. *J. Am. Chem. Soc.* **2011**, *133*, 4257.
(74) Bain, G. A.; Berry, J. F. *J. Chem. Educ.* **2008**, *85*, 532.
(75) Sur, S. K. *J. Magn. Reson.* **1989**, *82*, 169.
(76) Evans, D. F. *J. Chem. Soc.* **1959**, 2003.
(77) Frisch, M. J.; et al. *Gaussian 03, revision D.02*; Gaussian, Inc.: Wallingford CT, 2004.